



NIST  
PUBLICATIONS



United States Department of Commerce  
Technology Administration  
National Institute of Standards and Technology

*NISTIR 5055*

# Uncertainty in Null Polarimeter Measurements

---

---

K.B. Rochford  
C.M. Wang

C  
10  
156  
10.5055  
1996



*NISTIR 5055*

# Uncertainty in Null Polarimeter Measurements

---

---

K.B. Rochford  
C.M. Wang

Optoelectronics Division  
Electronics and Electrical Engineering Laboratory  
and  
Statistical Engineering Division  
Computing and Applied Mathematics Laboratory  
National Institute of Standards and Technology  
Boulder, Colorado 80303-3328

October 1996



---

U.S. DEPARTMENT OF COMMERCE, Michael Kantor, Secretary  
TECHNOLOGY ADMINISTRATION, Mary L. Good, Under Secretary for Technology  
NATIONAL INSTITUTE OF STANDARDS AND TECHNOLOGY, Arati Prabhakar, Director



# Uncertainty in Null Polarimeter Measurements

K. B. Rochford and C. M. Wang

National Institute of Standards and Technology  
325 Broadway, Boulder, CO 80303-3328

This Internal Report details the error analysis of a nulling polarimeter used for retardance measurements. We determined that the uncertainty arising from random effects is between  $0.07^\circ$  and  $0.10^\circ$  for measurements of several retarders with nominally  $90^\circ$  retardance. This instrument and two other methods were used to determine the retardance of a stable rhomb device proposed as a standard retarder. The measurement results were used to support certification of our retarder as a NIST Standard Reference Material.

Keywords: Fresnel rhomb; measurement; null polarimetry; polarimetry; polarization; retardance; standards; Standard Reference Materials; uncertainty analysis.

## 1. Introduction

A system commonly known as the manual null instrument [1] or nulling ellipsometer [2] was a secondary polarimetric method used for determining retardance in our efforts to develop a stable retarder [3,4]. For this measurement, a compensating quarterwave retarder (C) and the retarder under test (R) are placed between an input polarizer (P) and analyzing polarizer (A) (Figure 1). We illuminate the system with circular polarization so that the optical power incident on the compensator is constant as the azimuth of P is rotated. This circular input polarization is obtained using a linearly polarized (LP) optical beam and a Soleil-Babinet compensator (SBC) adjusted to quarterwave retardance.

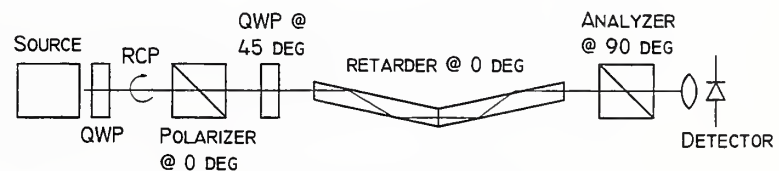


Figure 1. Schematic of null polarimeter apparatus.

To measure retardance, the system is aligned so that polarizers P and A are crossed (transmission axes are orthogonal) and the retardance axes of compensator C are coincident with the polarizer axes. The retardance axes of R are aligned at  $45^\circ$  to the polarizer axes. While the optical power exiting the system is monitored, polarizer P is rotated to the angle that yields the minimum detected power. The magnitude of polarizer rotation  $\alpha$  required to reach this null is equal to half the measured retardance  $\delta_m$  (or  $\delta_m = 2\alpha$ ).

This system benefits from the high accuracy with which transmission nulls can be determined. If the system were used without the compensator C, the output of retarder R would be elliptical, in general, and the null could be difficult to locate. For example, if R is a quarterwave retarder, the system's transmittance is constant for all positions of P if no compensator is used, and a null cannot be found. Because an appropriately aligned quarterwave retarder can convert any elliptical state into a linear state, component C causes the light incident on the polarizing analyzer to be linearly polarized, and this ensures a high-extinction null that can be accurately determined.

Generally, several parameters are important for a complete ellipsometric measurement. For example, the sign of the compensator's retardance (location of the fast axis) and the direction of polarizer's rotation are required to determine the sign of the retarder. In addition, the analyzer can be rotated to a null and provide a measure of diattenuation. For our purposes, however, these details were unimportant and ignored. First, the sign of the retardance is determined by the design of our rhomb retarder, and routine experimental determination is not needed. Second, the device is designed for negligible diattenuation, and this has been verified independently, so additional measurement is not necessary.

In this paper, we discuss the retardance errors associated with the null measurements made on five prototype stable retarders labeled SR1 through SR5.

## 2. Experimental Method

Each retardance measurement required several alignment, readout, and adjustment steps. The procedure used to obtain a retardance estimate  $\delta_m$  is discussed below. Also, several general concepts and practices are reviewed.

### 2.1 General Practices

- 2.1.1 As optical elements are inserted into the optical beam path, the elements are adjusted for normal incidence by monitoring the Fresnel reflection from the surface. For anti-reflection coated components, this was done using a collinear HeNe laser directed along the IR laser path.
- 2.1.2 "Nulling," or finding the polarizer/analyzer angle which yields maximum extinction, is performed several times over the course of a measurement. Two methods, creatively named "A" and "B," are described below:
  - Method A: The device (polarizer P or analyzer A) is manually rotated to the point of maximum extinction. The angle is read directly from the vernier on the rotation stage.
  - Method B: The device is rotated to a position that yields a predetermined transmittance (for example,  $T = 10^{-4}$ ), and the angle read directly from the stage and recorded. The device is then rotated through the null to a second point with the same transmittance, and this second angle recorded. This procedure may be repeated several times. The arithmetic mean is calculated, and the stage is rotated to the mean angle.
- 2.1.3 The procedure requires that the retardance axes of several components be found polarimetrically. When a retarder is placed between a crossed polarizer and analyzer, minimum transmission occurs when the retardance axes coincide with the polarizer/analyzer axes. Thus, rotating the retarder until the system output is nulled locates the retardance axes.
- 2.1.4 The input to the first polarizer is collimated, circularly polarized light from a laser diode. Collimated light was polarized and directed toward an analyzing polarizer (A), lens and linear photodetector aligned with the propagation axis (the Figure 1 setup with components P, C, and R removed from beam path). SBC is placed after the first polarizer, and its retardance axis located polarimetrically. The SBC's retardance axes are rotated  $45^\circ$ , and the retardance of the SBC is adjusted to quarterwave. Proper SBC adjustment is checked by measuring the modulation of detected power as the analyzer is rotated; there should be no modulation for perfect circular polarization. Once aligned, the optics for providing circular polarization were not routinely adjusted between retardance measurements.

## 2.2 Experimental Procedure

The procedure for measuring retardance consists of the seven steps described below:

- 2.2.1 A polarizer (P) is inserted into the system after the SBC. The transmission axis is aligned roughly perpendicular to the optical table, and the analyzer (A) is rotated to a transmission null (maximum extinction). The polarizer angle is read to obtain the initial angle  $\alpha_{10}$ . Nulling and reading are accomplished using either method A or B, which are used throughout the procedure and are described above (Section 2.1.2).
- 2.2.2 The retarder R is inserted into the system and its retardance axes found polarimetrically. Then the retarder is temporarily removed from the system. (The mounting hardware is sufficiently stable to allow extraction and reinsertion without significantly altering retarder alignment.)
- 2.2.3 The polarizer-analyzer pair are rotated  $45^\circ$  so that the polarizer-analyzer transmission axes bisect the retardance axes of R. The initial angle for retardance measurement becomes  $\alpha_1 = \alpha_{10} + 45^\circ$ .
- 2.2.4 The compensating quarterwave plate (C) is inserted near polarizer P. The compensator's retardance axes are aligned to coincide with the polarizer-analyzer axes.
- 2.2.5 The retarder is reinserted in between compensator C and analyzer A. Polarizer P is rotated to a transmission null which occurs at polarizer angle  $\alpha_2$ . The measured retardance  $\delta_{m1} = 2|\alpha_2 - \alpha_1|$ .
- 2.2.6 Components C and A are rotated  $90^\circ$  so that the measurement can be repeated. (This second measurement, when averaged with the results of the prior measurement, cancels the effect of optical activity in compensator C and has no detrimental effect on measurement accuracy.)
- 2.2.7 Polarizer P is rotated to a transmission null, and another  $\alpha_2$  is found. A second measured retardance  $\delta_{m2} = 2|\alpha_2 - \alpha_1|$  is calculated. The measured retardance of our specimen R is  $\delta_m = (\delta_{m1} + \delta_{m2})/2$ .

## 2.3 Experimental Limitations

This procedure uses real components that are imperfect or have limitations. Several of the component issues of interest follow:

- 2.3.1 The optical source is a packaged laser diode. The device is driven with constant current, but still undergoes changes in wavelength due to temperature, age, etc. We estimate the worst-case wavelength variation to be  $1.31 \pm 0.02 \mu\text{m}$ .
- 2.3.2 The input polarization is not perfectly circular. When light was incident upon a rotating polarizer, a worst-case modulation of 20% could be measured. This corresponds to a SBC retardance of  $90 \pm 6.4^\circ$ . (SBC retardance  $\delta_{SB} = \cos^{-1}[(I_{\max} - I_{\min})/(I_{\max} + I_{\min})] = \cos^{-1}[(1.0 - 0.8)/(1.0 + 0.8)]$ ).
- 2.3.3 The polarizers used in the systems are high quality calcite polarizers. For our measurements, the light leakage at extinction overwhelmed any detection noise, and the polarizers limit the null determination. The maximum extinction was found by measuring the minimum and maximum transmission through crossed polarizers with phase-sensitive detection. Four measurements of the

extinction ( $= I_{\min}/I_{\max}$ ) for the polarizers P and A yielded a mean of  $6.1 \times 10^{-7}$  with a standard deviation of  $1.9 \times 10^{-7}$ .

- 2.3.4 The retardance of compensating waveplate C was independently measured to be  $87.9^\circ$ . Including the effect of  $\pm 20$  nm wavelength variation, the range of the compensator's retardance is  $87.9 \pm 1.4^\circ$ .
- 2.4.5 The rotation stages used in the experiment were ruled with marks at each  $0.1^\circ$ . The rotation was read directly from etched lines on the rotating and fixed mounts (and not read through any geared mechanism or screw drive), so the measurements were free of backlash.

### 3. Mathematical Modeling

For optical systems that have no depolarizing components, the evolution of polarization can be satisfactorily modeled using Jones calculus [5]. The measurements of our rhomb retarders in the null polarimeter meet this requirement, and Jones calculus was used to model the ideal system and determine the uncertainty due to individual component imperfections and alignment uncertainty.

In Jones calculus, the change in the electric field, defined as the column vector  $[E_x, E_y]^T$ , is found by multiplying the input field vector by a  $2 \times 2$  matrix corresponding to an optical element. Thus the output vector  $E_0$  resulting from a field  $E_i$  propagating through optical elements X and Y (which have Jones matrices  $M_x$  and  $M_y$ ) is  $E_0 = M_y \times M_x \times E_i$ .

#### 3.1 Ideal Null System

For the ideal null system, the following Jones matrices and vectors adequately describe the components of interest:

- 3.1.1 Light entering the measurement system is circularly polarized with input field

$$E_i = \frac{1}{\sqrt{2}} \begin{bmatrix} 1 \\ i \end{bmatrix}. \quad (1)$$

- 3.1.2 Polarizer P at angle  $\alpha$  from origin

$$P = \begin{bmatrix} \cos^2(\alpha) & \sin(\alpha)\cos(\alpha) \\ \sin(\alpha)\cos(\alpha) & \sin^2(\alpha) \end{bmatrix}. \quad (2)$$

- 3.1.3 Compensator C with  $90^\circ$  retardance

$$C = \begin{bmatrix} e^{i\pi/4} & 0 \\ 0 & e^{-i\pi/4} \end{bmatrix}. \quad (3)$$

- 3.1.4 Retarder R rotated  $45^\circ$  with unknown retardance  $\delta_0$

$$RET = \begin{bmatrix} \cos(\delta_0/2) & i \sin(\delta_0/2) \\ i \sin(\delta_0/2) & \cos(\delta_0/2) \end{bmatrix}. \quad (4)$$

3.1.5 Analyzer A fixed at  $90^\circ$

$$A = \begin{bmatrix} 0 & 0 \\ 0 & 1 \end{bmatrix}. \quad (5)$$

The output field is found by matrix multiplication

$$E_0 = A \times RET \times C \times P \times E_i \quad (6)$$

and the output intensity is calculated from the vector  $E_0$  using  $I = E_x E_x^* + E_y E_y^*$ , where the asterisk denotes complex conjugation. For the ideal system described by the matrices above,

$$I = \frac{1 - (\sin(2\alpha) \sin(\delta_0) + \cos(2\alpha) \cos(\delta_0))}{4}. \quad (7)$$

The null occurs where  $dI/d\alpha = 0$ , or when  $\tan(2\alpha) = \tan(\delta_0)$ ; thus,  $\delta_0 = 2\alpha$  for the ideal system.

### 3.2 Measurement error due to individual component error

Several possible error sources, including component imperfections or alignment uncertainty, were identified after careful consideration of the null system. Each of these errors is analyzed by forming the Jones matrix corresponding to the component-alignment error and determining the effect on measured retardance. Six errors were identified and analyzed below:

3.2.1 Error due to offset in compensator retardance. If the compensator retardance is  $\pi/2 + \epsilon$ , the Jones matrix becomes

$$C = \begin{bmatrix} e^{i(\pi/2 + \epsilon)/2} & 0 \\ 0 & e^{-i(\pi/2 + \epsilon)/2} \end{bmatrix} \quad (8)$$

and the detected intensity as a function of polarizer position becomes  $I = (1 - \sin(2\alpha)\sin(\delta_0)\cos(\epsilon) - \cos(2\alpha)\cos(\delta_0))/4$ . Again the null occurs when the derivative  $dI/d\alpha = 0$ , or when  $\tan(2\alpha) = \tan(\delta_0)\cos(\epsilon)$ . Since the measured retardance  $\delta_m = 2\alpha$ ,  $\tan(\delta_m) = \tan(\delta_0)\cos(\epsilon)$ , and the retardance measurement error  $\Delta\delta = \delta_0 - \delta_m = \delta_0 - \tan^{-1}[\tan(\delta_0)\cos(\epsilon)]$ .

3.2.2 Error due to compensator misalignment. If the compensator retardance axes and polarizer-analyzer axes are misaligned by  $\epsilon$ , the Jones matrix for the compensator becomes

$$C = \begin{bmatrix} e^{i\pi/4} \cos^2(\epsilon) + e^{-i\pi/4} \sin^2(\epsilon) & i \sin(2\epsilon) \sin(\pi/4) \\ i \sin(2\epsilon) \sin(\pi/4) & e^{-i\pi/4} \cos^2(\epsilon) + e^{i\pi/4} \sin^2(\epsilon) \end{bmatrix}. \quad (9)$$

Again, we calculate the detected intensity  $I$  and find where the derivative  $dI/d\alpha = 0$ . This yields

$$\tan(2\alpha) = \frac{\cos(\delta_0) \sin(4\epsilon) + 2 \sin(\delta_0) \cos(2\epsilon)}{\cos(\delta_0) \cos(4\epsilon) - 2 \sin(\delta_0) \sin(2\epsilon) + \cos(\delta_0)}. \quad (10)$$

As before, the error in measured retardance  $\Delta\delta$  can be found by subtracting  $2\alpha$  ( $=\delta_m$ ) from  $\delta_0$ .

We have treated both retardance and alignment compensator errors as separate here and in Section 3.2.1. When both errors are taken together,

$$\tan(2\alpha) = \frac{\cos(\delta) \sin(4\epsilon_2) [1 + \sin(\epsilon_1)] + 2 \sin(\delta) \cos(\epsilon_1) \cos(2\epsilon_2)}{\cos(\delta) [\cos(4\epsilon_2) [\sin(\epsilon_1) + 1] - \sin(\epsilon_1) + 1] - 2 \sin(\delta) \sin(2\epsilon_2) \cos(\epsilon_1)}, \quad (11)$$

where  $\epsilon_1$  is the compensator retardance error and  $\epsilon_2$  is the alignment error.

For the errors  $\epsilon_{1,2}$  typical for our measurements, the retardance error found using eq (11) is equal to the sum of the separate errors (eq (10) and Section 3.2.1). We use the separate forms as this allows us to use different types of errors  $\epsilon$  in the calculation of uncertainty.

3.2.3 Error due to misaligned retarder. If the retarder is misaligned by an angle  $\epsilon$ , the appropriate Jones matrix is

$$RET = \begin{bmatrix} e^{-i\delta_0/2} \sin^2(\epsilon + \pi/4) + e^{i\delta_0/2} \cos^2(\epsilon + \pi/4) & i \sin(\delta_0/2) \cos(2\epsilon) \\ i \sin(\delta_0/2) \cos(2\epsilon) & e^{i\delta_0/2} \sin^2(\epsilon + \pi/4) + e^{-i\delta_0/2} \cos^2(\epsilon + \pi/4) \end{bmatrix}. \quad (12)$$

Calculating the derivative  $dI/d\alpha$  gives

$$\tan(2\alpha) = \frac{2 \sin(\delta_0) \cos(2\epsilon)}{\cos(4\epsilon) (\cos(\delta_0) - 1) + \cos(\delta_0) + 1}. \quad (13)$$

Measured retardance error  $\Delta\delta$  can be found by subtracting  $2\alpha$  ( $=\delta_m$ ) from  $\delta_0$ . This error causes a decrease in measured retardance for all cases of interest.

3.2.4 Error due to analyzer misalignment. If the analyzer is misaligned by an angle  $\epsilon$ , the Jones matrix becomes

$$A = \begin{bmatrix} \sin^2(\epsilon) & -\cos(\epsilon)\sin(\epsilon) \\ -\cos(\epsilon)\sin(\epsilon) & \cos^2(\epsilon) \end{bmatrix}. \quad (14)$$

Solving as before, we find that the dependence on  $\epsilon$  cancels and that  $\tan(2\alpha) = \tan(\delta)$ , the relationship for an ideal system. Thus, errors in analyzer position will not affect retardance measurements.

3.2.5 Error due to input polarization error. If the optical input to the system is not circularly polarized, errors can result when the null is found using method B. This occurs because the transmission through polarizer P does not vary symmetrically with polarizer angle if the input polarization is not circular.

This can be modeled by using an input field matrix that is a function of SBC retardance  $\delta_{SB}$

$$E_i = \frac{1}{\sqrt{2}} \begin{bmatrix} e^{i\delta_{SB}/2} & 0 \\ 0 & e^{-i\delta_{SB}/2} \end{bmatrix}. \quad (15)$$

To find the functional form of intensity as the polarizer rotates, we model the simpler system  $I = A \times P \times E_i$ , which yields  $I = \cos(\alpha)\sin^3(\alpha)\cos(\delta_{SB}) + \frac{1}{2}\sin^2(\alpha)$ . For  $I_{null}$  (which corresponds to the intensity at which angles on either side of the null are measured) and retardance  $\delta_{SB}$ , we can find the roots  $\alpha'$  and  $\alpha''$ . Comparing the average  $\alpha_m = (\alpha' + \alpha'')/2$  with the ideal value  $\alpha = \delta_{SB}/2$  gives the angular error caused by input polarization errors.

3.2.6 Error due to optical activity in compensator waveplate. The quarterwave compensator had a small amount ( $\ll 1^\circ$ ) of optical activity (or rotation). This was modeled using a Jones matrix for C that included both retardance and rotation. Though the analysis shows that significant error can occur when determining the retardance (Section 2.2.1 through 2.2.5), the sign of the error changes when the retardance is remeasured after rotating the compensator and analyzer by  $90^\circ$  (Section 2.2.6). Thus, averaging the two retardance measurements cancels this error, and the null measurement is insensitive to optical activity in the compensator.

#### 4. Analysis of Measurement Uncertainties

We can calculate retardance uncertainty for each step of a retardance measurement. As slightly different component values were used for individual measurements, retardance uncertainty for individual rhombs is listed as required.

##### 4.1 General uncertainties

The measurement of retardance requires the measurement of rotation angles as well as accurate rotation of a components to specified angles. We denote the calculated angle uncertainty by  $\epsilon_x$ , where the subscript x labels the source of error.

4.1.1 Stage resolution. The rotation stages used for these measurements were ruled every  $0.1^\circ$  and were read from the overlap of graduations on two ruled pieces (one fixed vernier, and one rotating scale). We assume that during readout we can resolve reading within  $\pm 0.05^\circ$ , or halfway between the graduations. The uncertainty is estimated by assuming that the readout has a uniform error over of a width of  $0.05^\circ$ . With this model, the standard angle uncertainty (one standard deviation) is  $\epsilon_R = 0.05^\circ/\sqrt{12} = 0.0144^\circ$ .

4.1.2 Method A nulling. Transmission nulling using method A is limited by polarizer imperfections. Ideally, the transmittance  $T = \sin^2\theta$ , where  $\theta$  is the angle from extinction. For our polarizers, the best extinction obtained was  $T = 6.1 \times 10^{-7}$  with a standard deviation of  $1.9 \times 10^{-7}$  based on four measurements. Thus corresponds to an angle resolution of  $0.045^\circ$  (with a standard error of 0.0035). We calculate the maximum angle uncertainty ( $3\sigma$ ) as the mean angle resolution plus 3 standard errors ( $0.045^\circ + 3 \cdot 0.0035^\circ = 0.0555^\circ$ ), so the standard uncertainty for nulling  $\epsilon_A = 0.0185^\circ$ .

For some cases, the nulling angle must be read out for calculation or angle adjustment. In this case, we combine the nulling and readout uncertainty to form  $\epsilon_{AR} = (\epsilon_A^2 + \epsilon_R^2)^{1/2} = 0.0235^\circ$ .

4.1.3 Method B nulling. Transmission nulling using method B is more complicated because of input polarization uncertainty (which is due to uncertainty in the SB compensator retardance). If the null is found by locating the angles at which the transmittance is  $I_{null}$  when the compensator retardance is  $\delta_{SB}$  (Section 3.2.5), the worst-case uncertainty  $\Delta\epsilon_{SB} = (\alpha' + \alpha'')/2$  where  $\alpha'$  and  $\alpha''$  are the roots of  $\cos(\alpha)\sin^3(\alpha)\cos(\delta_{SB}) + \frac{1}{2}\sin^2(\alpha) - I_{null} = 0$ . The angle uncertainty due to input polarization is  $\epsilon_{SB} = \Delta\epsilon_{SB}/3$ . Because the values of  $I_{null}$  differed among the various measurements, its values and corresponding  $\epsilon_{SB}$  are tabulated in Table 1 for  $\delta_{SB} = 90 \pm 6.4^\circ$ .

Table 1. Angular uncertainty due to input polarization errors.

Device	Maximum $I_{null}$	Roots (rad)	$\Delta\epsilon_{SB} (^\circ)$	$\epsilon_{SB} (^\circ)$
SR1	$2.44 \times 10^{-5}$	0.00698, -0.00699	$2.86 \times 10^{-4}$	$9.55 \times 10^{-5}$
SR2	$5.95 \times 10^{-5}$	0.01090, -0.01092	$5.73 \times 10^{-4}$	$1.91 \times 10^{-4}$
SR3	$1.52 \times 10^{-4}$	0.01740, -0.01747	$2.01 \times 10^{-3}$	$6.68 \times 10^{-4}$
SR4	$1.05 \times 10^{-3}$	0.04561, -0.04608	$1.35 \times 10^{-2}$	$4.49 \times 10^{-3}$
SR5	$4.40 \times 10^{-4}$	0.02957, -0.02977	$5.73 \times 10^{-3}$	$1.91 \times 10^{-3}$

In addition to uncertainty  $\epsilon_{SB}$ , additional uncertainty results from the readout process; the two angular positions of  $I_{null}$  must be read, and the stage then rotated to the average of these two angles. These uncertainties can be combined to form the total uncertainty for nulling using method B,  $\epsilon_B = (\epsilon_{SB}^2 + 3\epsilon_R^2/2)^{1/2}$ . Table 2 lists the resulting uncertainty for each device.

Table 2. Angle uncertainty from method B nulling.

	SR1	SR2	SR3	SR4	SR5
$\epsilon_B$	0.0177	0.0177	0.0177	0.0182	0.0178

## 4.2 Angle Measurement Uncertainty Arising from Experimental Limitations

Each retardance measurement has several steps requiring reading and/or adjustments of the rotation angles of various system components. In this section, we list the uncertainties arising at each step in order of occurrence. (For reference, the analysis is numbered to correspond with the procedural steps described in Section 2.2.)

- 4.2.1 Null polarizer-analyzer and readout angle  $\alpha_1$ . Both nulling methods were used in determining  $\alpha_1$  for individual measurements. Also, one determination (SR4) used the average of two measurements. The angle uncertainty associated with this step is either  $\epsilon_{AR}$  or  $\epsilon_B$ , depending on the nulling method used. For N measurements, the angle uncertainty  $\epsilon_1 = \epsilon_{AR,B}/N^{1/2}$ . The methods and results are tabulated in Table 3.

Table 3. Angle uncertainty in polarizer-analyzer readout.

	SR1	SR2	SR3	SR4	SR5
Null method	A	B	A	B	B
N	1	1	1	2	1
$\epsilon_1$	0.0235	0.0177	0.0235	0.0129	0.0178

- 4.2.2 Location of the retardance axes of R. Method A was used for each determination. Thus, the angle uncertainty associated with axis determination is  $\epsilon_2 = \epsilon_A = 0.0185^\circ$ .

- 4.2.3 45° rotation of polarizer/analyzer. This step requires a rotation of 45° with respect to the retarder axes, so rotation causes an effective uncertainty in the location of these axes. The uncertainty of retarder axis angle  $\epsilon_2$  and a polarizer/analyzer readout with angular uncertainty  $\epsilon_R$  are combined. The combined error for the retarder axes after the polarizer / analyzer rotation is  $\epsilon_{RET} = (\epsilon_2^2 + \epsilon_R^2)^{1/2} = 0.0235$  for all measurements.

In addition, the angle of the polarizer with respect to the analyzer accrues uncertainty during the rotation because of the initial nulling limitation and readout error from rotation. The combined angle uncertainty between the polarizer and analyzer is  $\epsilon_{P/A} = (\epsilon_1^2 + \epsilon_R^2)^{1/2}$ . Table 4 lists the resulting uncertainties.

Table 4. Angle uncertainty due to polarizer/analyzer misalignment.

	SR1	SR2	SR3	SR4	SR5
$\epsilon_{P/A}$	0.0275	0.0228	0.0275	0.0194	0.0229

- 4.2.4 Location of compensating waveplate's retardance axes. The determination of the waveplate's axes was made using different methods, and the resulting angle uncertainty  $\epsilon_4$  equals  $\epsilon_A$  or  $\epsilon_B$ , depending on the nulling method used. In one case, two measurements were made so the uncertainty is reduced by  $2^{-1/2}$ . The resulting angle uncertainty for each case is tabulated in Table 5.

Table 5. Angle uncertainty in waveplate axis determination.

	SR1	SR2	SR3	SR4	SR5
Null method	A	A	A	B	B
N	1	1	1	1	2
$\epsilon_4$	0.0185	0.0185	0.0185	0.0182	0.0126

- 4.2.5 Rotation of polarizer to null to find  $\alpha_2$  and  $\alpha_2 - \alpha_1$ . Null method B was used for each measurement so the null angle uncertainty =  $\epsilon_B$  for each case. Multiple measurements were made in several cases, so the effective angle uncertainty  $\epsilon_5 = \epsilon_B/N^{1/2}$ . The difference  $\alpha_2 - \alpha_1$  is of interest, and the combined uncertainty is  $\epsilon_{\Delta\alpha} = (\epsilon_5^2 + \epsilon_1^2)^{1/2}$ . Table 6 lists the calculated angle uncertainties for finding  $\alpha_2$ .

Table 6. Angle uncertainty for polarizer rotation to null.

	SR1	SR2	SR3	SR4	SR5
N	3	3	1	3	3
$\epsilon_5$	0.0102	0.0102	0.0177	0.0105	0.0103
$\epsilon_{\Delta\alpha}$	0.0256	0.0204	0.0294	0.0167	0.0205

- 4.2.6 Rotation of biasing waveplate to repeat measurement. The quarterwave compensator and analyzer are rotated  $90^\circ$ . Compensator rotation introduces readout uncertainty  $\epsilon_R$  and an angle uncertainty  $\epsilon_4$  due to the initial alignment of the compensator. These uncertainties combine to form an angle uncertainty for the compensator position,  $\epsilon_6 = (\epsilon_R^2 + \epsilon_4^2)^{1/2}$ . The uncertainty in analyzer rotation does not contribute to retardance uncertainty (see Section 3.2.4) and can be ignored. The values for  $\epsilon_6$  are tabulated in Table 7.

Table 7. Angle uncertainty in compensator position.

	SR1	SR2	SR3	SR4	SR5
$\epsilon_6$	0.0235	0.0235	0.0235	0.0233	0.0191

- 4.2.7 Remeasurement of nulling angle  $\alpha_2$  and  $\alpha_2 - \alpha_1$ . As in Section 4.2.5, the nulling angles are all measured by method B so the angle uncertainty is  $\epsilon_B$ . Multiple measurements were made in several cases, so the effective angle uncertainty  $\epsilon_7 = \epsilon_B/N^{1/2}$ . The difference  $\alpha_2 - \alpha_1$  is of interest, and the combined uncertainty is  $\epsilon_{\Delta\alpha'} = (\epsilon_7^2 + \epsilon_1^2)^{1/2}$ . Table 8 lists the calculated angle uncertainties.

Table 8. Angle uncertainty for second rotation to polarizer null.

	SR1	SR2	SR3	SR4	SR5
N	2	4	1	3	3
$\epsilon_7$	0.0125	0.0088	0.0177	0.0105	0.0103
$\epsilon_{\Delta\alpha'}$	0.0266	0.0198	0.0294	0.0167	0.0205

### 4.3 Uncertainty in Measured Retardance

The angle uncertainties and component value errors or uncertainties combine to yield uncertainty in the measurement of retardance. Some of the uncertainties depend on the retardance itself, and the measured retardance  $\delta_m$  is used for this estimate. Because the uncertainties are generally small, the uncertainty estimate is not greatly affected by using the measured value in our calculations and recursive estimation is not needed. The standard retardance uncertainty  $u$  ( $= \delta_m - 2\alpha$ , where  $2\alpha$  is the measured retardance expected from the error equations, and  $\delta_0 = \delta_m$  as needed) are discussed below.

- 4.3.1 Retardance uncertainty due to retarder / polarizer misalignment. The retardance uncertainty  $u_{RET}$  due to retarder misalignment is found using eq (12) from Section 3.2.3 and the angle uncertainty  $\epsilon_{RET} = 0.0235$ . The uncertainty for each retardance measurement is listed in Table 9.

Table 9. Retardance error due to retarder misalignment.

	SR1	SR2	SR3	SR4	SR5
$\delta_m$	89.2	89.41	89.4	87.89	89.35
$u_{RET}$	$4 \times 10^{-5}$				

The resulting error is a bias, and causes the measured retardance to be slightly less than the true value. (As discussed in Section 3.2.2, treating compensator error components individually can understate the total uncertainty unless the component uncertainties are summed. Clearly, the uncertainty is negligible for our case, and our separation of the errors poses no problem.)

- 4.3.2 Retardance uncertainty due to compensator retardance uncertainty. This uncertainty depends on the specimen retardance and the compensator retardance uncertainty. We estimate a maximum compensator uncertainty of  $3.5^\circ$  (Section 2.3.4), so application of the error equation in Section 3.2.1 yields a maximum uncertainty  $\Delta\delta_{CR}$ . The maximum uncertainty and standard uncertainty  $u_{CR} = \Delta\delta_{CR}/3$  is tabulated in Table 10.

Table 10. Retardance uncertainty due to compensator retardance uncertainty.

	SR1	SR2	SR3	SR4	SR5
$\Delta\delta_{CR}$	$1.49 \times 10^{-3}$	$1.1 \times 10^{-3}$	$1.12 \times 10^{-3}$	$3.92 \times 10^{-3}$	$1.21 \times 10^{-3}$
$u_{CR}$	$4.97 \times 10^{-4}$	$3.67 \times 10^{-4}$	$3.73 \times 10^{-4}$	$1.31 \times 10^{-3}$	$4.03 \times 10^{-4}$

The uncertainty is a bias that causes the measured retardance to be slightly less than the true value.

- 4.3.3. Retardance uncertainty due to compensator misalignment. The compensator misalignment  $\epsilon_4$  directly alters the retardance measurement with standard uncertainty  $u_{CA1}$  found using eq (10) and  $\delta_m$ . Interestingly, numerical evaluation of the error yields  $u_{CA1} = 2\epsilon_4$ . Table 11 lists the resulting uncertainties.
- 4.3.4 Retardance uncertainty due to  $\Delta\alpha$  determination uncertainty. The retardance is measured by direct measurement of the magnitude of polarizer rotation  $\Delta\alpha$  (Sections 2.2.5 and 2.2.7). Since  $\delta_m$

$= 2\Delta\alpha$ , the standard uncertainty is  $u_{PR1} = 2\epsilon_{\Delta\alpha}$ . Table 11 lists the standard uncertainty for each measurement.

- 4.3.5 Retardance uncertainty due to compensator misalignment (second measurement). Uncertainty is calculated as in Section 4.3.3; again numerical evaluation shows that the compensator misalignment directly alters the retardance measurement. For the second measurement, additional uncertainty accrues (Section 4.2.6), and the resulting standard retardance uncertainties  $u_{CA2} = 2\epsilon_6$  are listed in Table 11.
- 4.3.6 Retardance uncertainties due to  $\Delta\alpha$  determination uncertainty (second measurement). The retardance is again measured by direct measurement of the magnitude of polarizer rotation  $\Delta\alpha$  (Section 4.2.7) and the standard uncertainty is  $u_{PR2} = 2\epsilon_{\Delta\alpha}$  (Table 11).

Table 11. Retardance uncertainty arising from  $\Delta\alpha$  error.

	SR1	SR2	SR3	SR4	SR5
$u_{CA1}$	0.0370	0.0370	0.0370	0.0365	0.0252
$u_{PR1}$	0.0512	0.0408	0.0588	0.0333	0.0411
$u_{CA2}$	0.0469	0.0469	0.0469	0.0465	0.0382
$u_{PR2}$	0.0532	0.0395	0.0588	0.0333	0.0411

## 5. Analysis of Rhomb Retardance Uncertainty

In addition to uncertainty introduced by our null measurement instrument, there are retardance uncertainties that arise from the retarder itself. Our stable rhomb, while more nearly achromatic and angle insensitive than typical retarders, exhibits small retardance changes with wavelength and incident angle. An estimate of these changes is important because these devices were blindly measured by each of three independent methods to ensure the reproducibility and accuracy of our measurement techniques. Uncertainties due to rhomb retardance changes are estimated below.

### 5.1 Retardance Uncertainty Due to Input Angle

The angle of total internal reflection (TIR) inside the rhomb is  $\theta_1 = \alpha_R + \sin^{-1}(\sin(\beta)/n)$ , where  $\alpha_R$  is the acute angle of the rhomb,  $\beta$  is the angle deviation from normal incidence at the input face, and  $n$  is the refractive index of the rhomb. Our device is made with two rhombs; for the two reflections in the first rhomb the TIR angle is  $\theta_1$ , while the second two reflections in the second rhomb have TIR angle  $\theta_2 = \alpha_R - \sin^{-1}(\sin(\beta)/n)$ . The retardance  $R$  upon TIR is given by Fresnel's equations and can be written as

$$R(\theta) = 2 \tan^{-1} \left( \frac{\sqrt{\sin^2(\theta) - 1/n^2} \cos(\theta)}{\sin^2(\theta)} \right). \quad (16)$$

The total rhomb retardance is then  $2R(\theta_1) + 2R(\theta_2)$ , and the retardance error due to input angle error  $\beta$  is  $\Delta\delta = 2R(\theta_1) + 2R(\theta_2) - 4R(\alpha_R)$ .

At 1.32  $\mu\text{m}$ ,  $n \approx 1.805$  for the glass used in out rhombs [4]. We estimate the maximum  $\beta$  by assuming that the rhomb can be aligned using back-reflection of an incident beam with a resolution of one beam diameter. For a nominal path of 50 cm, and a maximum beam diameter of 3 mm, the maximum input angle uncertainty  $\beta_{\text{max}} = \tan^{-1}(3/500) = 0.006$  rad. The acute angles  $\alpha_R$  at which each rhomb was cut and corresponding uncertainty estimates  $u_\beta$  are listed in Table 12. The standard uncertainty is one-third the maximum uncertainty resulting from  $\beta_{\text{max}}$ .

Table 12. Acute angles and input angle uncertainty for measured rhombs.

Device	angle $\alpha_R$ ( $^\circ$ )	$\Delta\delta$ ( $^\circ$ )	$u_\beta$ ( $^\circ$ )
SR1	76.375		
SR2, SR3	76.391	$4.17 \times 10^{-4}$	$1.4 \times 10^{-4}$
SR4, SR5	76.366		
SR6	76.295	$4.21 \times 10^{-4}$	$1.4 \times 10^{-4}$

Positive and negative values of input angle  $\beta$  both decrease the retardance of the rhomb.

## 5.2 Retardance Uncertainty Due to Wavelength Changes

Using the Sellmeier equation for refractive index [3] and eq (16), we can estimate the rhomb retardance at various wavelengths. For a maximum wavelength variation of  $\pm 20$  nm about a center wavelength of 1310 nm, the maximum retardance change is  $\pm 0.0105^\circ$  and the standard uncertainty is  $u_\lambda = 0.0035^\circ$ .

## 5.3 Retardance uncertainty due to error in rhomb alignment

The stable retarder is made by attaching two rhombs with retardance  $\delta_\rho/2$ . During the alignment it is possible to include a small rotation, or twist,  $\epsilon_t$ , between the devices. Twist causes an error in the retarder alignment  $\epsilon_{\text{RET/T}} = -\frac{1}{2}\epsilon_t$ , since the nulling angle between crossed polarizers is found with less resolution; this value is generally different than the error  $\epsilon_{\text{RET}} = 0.0235^\circ$  due to polarizer extinction and rotation errors (Section 4.2.3). The resulting retardance error  $u_{\text{RET}}$  is calculated from the equations in Section 3.2.3 as before and tabulated in Table 13.

Table 13. Uncertainty due to twist in rhomb.

	SR1	SR3	SR4	SR2	SR5
$\epsilon_t$	$0.36^\circ$	$0.6^\circ$	$0.72^\circ$	$0.24^\circ$	$0.2^\circ$
$\epsilon_{\text{RET/T}}$	$0.18^\circ$	$0.3^\circ$	$0.36^\circ$	$0.12^\circ$	$0.1^\circ$
$u_{\text{RET}}$	$2.2 \times 10^{-3^\circ}$	$6.3 \times 10^{-3^\circ}$	$8.9 \times 10^{-3^\circ}$	$1.0 \times 10^{-3^\circ}$	$6.9 \times 10^{-4^\circ}$

These values are larger than the  $u_{\text{RET}}$  values calculated from polarizer errors in Section 4.2.3; we will use these larger values in the combined uncertainty calculations below.

## 6. Net retardance uncertainty from measurements using null method

We now combine the various retardance uncertainties previously discussed.

## 6.1 Retardance Measurement Uncertainty Arising from Effects that Bias Retardance

Retarder misalignment ( $u_{RET}$ , Section 4.3.1) and compensator retardance uncertainty ( $u_{CR}$ , Section 4.3.2) cause measurement biases that result in a retardance estimate that is slightly less than the true value. Similarly, input angle uncertainty ( $u_{\beta}$ , Section 5.1) also decreases retardance. These are combined using the root-sum-of-squares (RSS) method to give the combined uncertainty  $u_{C/S}$  arising from biasing. Table 14 lists these values.

Table 14. Uncertainty arising from systematic effects.

	SR1	SR2	SR3	SR4	SR5
$u_{RET}$	$2.2 \times 10^{-3}$	$1.0 \times 10^{-3}$	$6.3 \times 10^{-3}$	$8.9 \times 10^{-3}$	$6.9 \times 10^{-4}$
$u_{CR}$	$4.97 \times 10^{-4}$	$3.67 \times 10^{-4}$	$3.73 \times 10^{-4}$	$1.31 \times 10^{-3}$	$4.03 \times 10^{-4}$
$u_{\beta}$	$1.4 \times 10^{-4}$				
$u_{C/S}$	$2.6 \times 10^{-3}$	$1.1 \times 10^{-3}$	$6.3 \times 10^{-3}$	$9.0 \times 10^{-3}$	$8.1 \times 10^{-4}$

## 6.2 Retardance Measurement Uncertainty Arising from Random Effects

Random uncertainties arise from compensator misalignment ( $u_{CA1}$  and  $u_{CA2}$ , Sections 4.3.3 and 4.3.5),  $\Delta\alpha$  determination ( $u_{PR1}$  and  $u_{PR2}$ , Sections 4.3.4 and 4.3.6), and wavelength variation ( $u_{\lambda}$ , Section 5.2). These are tabulated in Table 15, and the combined uncertainties due to random effects for each measurement,  $u_{C/R1}$  and  $u_{C/R2}$ , are calculated using RSS. The measure retardance  $\delta_m$  is the mean of these two measured values, and the combined uncertainty for these two measurements gives the combined standard uncertainty from random effects,  $u_{C/R} = \frac{1}{2}(u_{C/R1}^2 + u_{C/R2}^2)^{1/2}$ . The results are listed in Table 15.

Table 15. Uncertainty arising from random effects.

	SR1	SR2	SR3	SR4	SR4
$u_{CA1}$	0.0370	0.0370	0.0370	0.0365	0.0252
$u_{PR1}$	0.0512	0.0408	0.0588	0.0333	0.0411
$u_{\lambda}$	0.0035	0.0035	0.0035	0.0035	0.0035
$u_{C/R1}$	0.0633	0.0552	0.0695	0.0495	0.0483
$u_{CA2}$	0.0469	0.0469	0.0469	0.0465	0.0383
$u_{PR2}$	0.0532	0.0395	0.0588	0.0333	0.0411
$u_{C/R2}$	0.0709	0.0614	0.0752	0.0572	0.0561
$u_{C/R}$	0.0475	0.0413	0.0512	0.0379	0.0371

### 6.3 Reported Uncertainty for Null Measurements

Comparison of Tables 14 and 15 shows that systematic uncertainty  $u_{C/S}$  is negligible compared to the standard uncertainty  $u_{C/R}$  arising from random effects for devices SR1, SR2, and SR5, so correction of the retardance measurement using  $u_{C/S}$  will not be attempted. For SR3 and SR4 the value  $u_{C/S}$  will be added to the measured retardance value as a correction. The combined standard uncertainty  $u_C$  for these measurements is  $u_{C/R}$ . Because  $u_{C/R}$  is much larger than the correction  $u_{C/S}$  added to the retardance values of SR3 and SR4, we consider the uncertainty from the correction to be negligible. In Table 16 the results of our prototype SRM retardance measurements using the null method are listed. In this Table, the number following the  $\pm$  symbol is the expanded uncertainty  $U = ku_C$ , where a coverage factor  $k = 2$  is used. If the uncertainty is approximately normally distributed with approximate standard deviation  $u_C$ , the value of retardance lies within the interval defined by  $U$  with a confidence level of approximately 95% [6].

Table 16. Results of retardance measurements using null method.

	SR1	SR2	SR3	SR4	SR5
Retardance ( $^\circ$ )	$89.2 \pm 0.1$	$89.41 \pm 0.08$	$89.41 \pm 0.10$	$87.90 \pm 0.08$	$89.35 \pm 0.07$

### 7. Conclusions

Measurements of a stable retarder using a manual null polarimeter have an expanded uncertainty  $U \leq 0.1^\circ$ . The system is fairly easy to align and operate, though two components are wavelength sensitive and must be changed if measurements at other wavelengths are required. Angle readout limitations of the rotation stages used in our system contribute the largest error sources, and this could be mitigated by improved stage resolution through automation (encoded stepper-motor driven stages, for example).

The retardance measurements used in this uncertainty analysis were performed by Ian Clarke (now at Galileo Electro-optics, Sturbridge, MA) during his visit as a Guest Scientist. We gratefully acknowledge his work on his project.

### 8. References

- [1] Tompkins, H.G. A user's guide to ellipsometry. Academic, Boston : 26-30; 1993.
- [2] Azzam, R.M.; Bashara, N.M. Ellipsometry and polarized light. North-Holland, Amsterdam: 166-169; 1977.
- [3] Rochford, K.B.; Williams, P.A.; Rose, A.H.; Clarke, I.G.; Hale, P.D.; Day, G.W. Standard polarization components: progress toward an optical retardance standard, in *Polarization analysis and measurement II*, Proc. SPIE 2265: 2-8; 1994.
- [4] Rochford, K.B.; Rose, A.H.; Williams, P.W.; Wang, C.M.; Clarke, I.G.; Hale, P.D.; Day, G.W. Design and performance of a stable linear retarder. Submitted to Applied Optics.
- [5] For example, see Kliger, D.S., Lewis, J.W.; Randall, C.E. Polarized light in optics and spectroscopy. Academic, Boston; 1990.
- [6] Taylor, B.N.; Kuyatt, C.E. Guidelines for evaluating and expressing the uncertainty of NIST measurement results. Natl. Inst. Stand. Technol. Tech. Note 1297; 1994.





